Generalization of Berreman's model to the case of large amplitude of the grooves

Generalization of Berreman's model to the case of large amplitude of the grooves

G. Barbero,[1] A. S. Gliozzi,[1] M. Scalerandi,[1] and L. R. Evangelista[2]
[1]*Dipartimento di Fisica del Politecnico, Corso Duca degli Abruzzi, 24-10129 Torino, Italy*
[2]*Departamento de Física, Universidade Estadual de Maringá, Avenida Colombo, 5790-87020-900 Maringá, Paraná, Brazil*
(Received 13 December 2007; revised manuscript received 4 April 2008; published 19 May 2008)

We generalize Berreman's model to the case $qA \geq 1$, where q is the wave vector of the surface structure and A its amplitude, to describe the alignment induced by a solid surface on a nematic liquid crystal. We show that, by taking into account correctly the elastic contribution to the surface energy connected with the surface topography, the effective surface energy is smaller than the one determined by Berreman, where the limiting surface is assumed flat and $qA \ll 1$. The analysis is performed by assuming that the anchoring energy on the surface is strong, i.e., nematic molecules in contact with the limiting surface are tangent to it, for any bulk distortion. The generalization to the weak anchoring case is also presented.

DOI: 10.1103/PhysRevE.77.051703 PACS number(s): 61.30.Hn, 61.30.Dk

I. INTRODUCTION

Long ago Berreman studied the contribution of elastic origin to the surface energy of a nematic liquid crystal [1] in the presence of a nonflat surface. In his analysis he considered a rubbed surface, and assumed that, in a first approximation, it can be approximated by a sinusoidal wave of wave vector $q=2\pi/\lambda$ and amplitude A, where λ is the spatial periodicity of the surface. In this framework, by assuming that $qA \ll 1$ and that $K_{11}=K_{22}=K_{33}=K$ [2], he showed that the surface topography is responsible for an equivalent anchoring energy

$$w_B = \frac{1}{2}K(qA)^2 q, \tag{1}$$

characterized by an easy direction parallel to the grooves. Equation (1) holds in the case where the surface is such as to fix the orientation of the nematic molecules parallel to the substrate (strong anchoring hypothesis). Berreman's model has been generalized, always by assuming $qA \ll 1$, first by Faetti [3], who investigated how a finite polar anchoring and reduced (or increased) surface order can affect the azimuthal anchoring, by proposing a more general expression for this quantity at a grooved surface. Subsequently, Fournier and Galatola [4], by means of a coarse-grained technique, derived an effective anchoring energy of a nematic liquid crystal in contact with a macroscopically corrugated surface, by including the anisotropy of elastic constants, absent in the original Berreman approach. Very recently, the model has been reexamined by Fukuda *et al.* [5], who showed that, at variance with the assumption made in the original approach of Berreman, the azimuthal distortion of the director cannot be considered as negligibly small. They showed, still working to the leading order in qA, that the anchoring energy depends on the fourth power of the sine of the angle made between the director at infinity and the direction of the surface grooves.

Numerous other studies have been carried out to understand the geometrical effects and to control the alignment of liquid crystal molecules on inhomogeneous or nanotextured surfaces [6–11] or, in general, to understand the effect of the surface topography on the molecular orientation of liquid-crystalline phases [12–15]. In recent years, the problem has become of practical importance, since photoalignment techniques have been developed as a convenient method to homogeneously align liquid crystals [16–18]. Rubbing of the substrate causes both elastic energy anisotropy, due to the morphology of the surface [19,20], and anisotropic interaction between the liquid-crystal molecules and the alignment layer surface [21]. In these cases, the solution suggested by Berreman is no longer valid, since $qA > 1$. This is e.g., the case of the competitive effects of grooves and photoalignment on nematic liquid-crystal alignment using azobenzene polymer where $qA \sim 2$ [22].

Here, we generalize the solution of Berreman to the case $qA > 1$, by solving the exact Laplace equation with the correct boundary conditions. We also compare the exact results with different approximations, either in the boundary conditions or in the definition of the surface profile. Our analysis indicates that the solution given by Berreman always overestimates the equivalent anchoring energy of the system. In Sec. II, we generalize the analysis of Berreman, valid in the strong anchoring hypothesis, to the case of large amplitude of the grooves. In Sec. III, we consider the case of weak anchoring. Section IV is devoted to the conclusions.

II. STRONG ANCHORING

Let us consider a nematic sample limited by a grooved surface. The direction of the grooves is parallel to the y axis of a Cartesian reference frame. We neglect here azimuthal variations of the director, i.e., those orthogonal to the x-z plane. Therefore, our sample can be considered as a two-dimensional (2D) specimen (in the x-z plane) with a surface profile described by

$$z_0(x) = A[1 + \cos(qx)]. \tag{2}$$

We assume that on the surface the anchoring is planar and strong. This means that the nematic director at the surface is parallel to the local geometrical tangent of the surface profile for all bulk distortions. We assume, furthermore, that the sample is infinite in the z direction. The bulk energy density, in the one-constant approximation, is given by

$$f[\theta(x,z)] = \frac{1}{2}K(\theta_{,x}^2 + \theta_{,z}^2), \tag{3}$$

where θ is the angle formed by the nematic director $\mathbf{n}$ with the x axis, $\theta_{,x}=\partial\theta/\partial x$, $\theta_{,z}=\partial\theta/\partial z$, and K is the elastic constant of the nematic liquid crystal [2]. The total elastic energy of one period is

$$F = \int_0^{\lambda}\int_0^{\infty} f[\theta(x,z)]dx\,dz. \tag{4}$$

The actual $\theta=\theta(x,z)$ field is the one minimizing F given by Eq. (4) [23]. Simple calculations show that $\theta=\theta(x,z)$ is a solution of the equation of Laplace,

$$\theta_{,xx} + \theta_{,zz} = 0, \tag{5}$$

and has to satisfy the boundary conditions

$$\theta_0(x) = \theta[x,z_0(x)] = \arctan[-qA\,\sin(qx)] \tag{6}$$

and

$$\lim_{z\to\infty} \theta(x,z) = 0. \tag{7}$$

Equation (5) states that in the configuration of equilibrium the bulk density of the mechanical torque vanishes, whereas the boundary condition (6) is connected with the hypothesis of strong anchoring, according to which the surface treatment is such as to impose the tangential orientation on the nematic molecules. Finally, Eq. (7) defines the transversality condition for the functional (4), and physically means that the mechanical torque has to vanish at infinity, where the system in not distorted [23]. Usually, distortions in the orientation of the nematic molecules vanish within a distance of a few wavelengths from the surface.

Equation (5) and the corresponding boundary conditions can be greatly simplified in the limit $qA\to 0$, when an analytical solution is possible [1]. On the contrary, for $qA>1$, the usual analysis in which the solution of Eq. (5) is in the form

$$\theta(x,z) = \sum_{n=0}^{\infty} M_n \sin(nqx)\exp(-nqz) \tag{8}$$

is no longer practicable. The problem in the determination of M_n is that the functions $u_n(x)=\sin(nqx)\exp[-nqz_0(x)]$ are not orthogonal. A solution can still be given by means of an orthogonalization procedure as discussed in Refs. [24,25]. However, the coefficients M_n obtained in this manner are not monotonically decreasing with increasing n. Therefore, to obtain an analytical solution, the usual orthogonalization methods require the calculation of an undefined (*a priori*) number of terms in the expansion.

A numerical solution of the problem is possible, in which we found the $\theta(x,z)$ field of equilibrium by solving the dynamical equation

$$K(\theta_{,xx} + \theta_{,zz}) = \eta\ \ \theta_{,t}, \tag{9}$$

where η is the bulk viscosity. Periodic (along x) boundary conditions are used, while fixed alignment of the molecules is defined on the lower surface of the specimen (where the profile is defined), according to Eq. (6). For the numerical solution, the second boundary condition (7) is automatically satisfied, provided the specimen depth (along z) is sufficiently large (about five wavelengths).

To find the actual solution corresponding to the equilibrium state, we let the system evolve until equilibrium, defined by $\theta_{,t}=0$, is reached. Using the equilibrium configuration $\theta(x,z)=\lim_{t\to\infty}\theta(x,z;t)$, we calculate the bulk energy density f by means of Eq. (3), and the total elastic energy F using Eq. (4). Finally, the equivalent anchoring energy strength is evaluated according to the relation

$$w = 2\frac{F}{\lambda}. \tag{10}$$

One may argue whether, when the amplitude of the grooves is large, it is possible to describe the anchoring energy by the effective anchoring energy defined in (10). In fact, the "effective" anchoring energy, if any, could possibly be more complicated in this general situation. However, our main concern here is just to analyze the validity of the Berreman model for arbitrary amplitude of the grooves, using, in this calculation, the original definition of the equivalent anchoring energy. Having this purpose in mind, we now estimate the equivalent anchoring energy calculating numerically the exact solution of Eq. (5). Furthermore, in order to estimate the validity of different approximations in which an analytical solution is possible, we solve Eq. (5) with modified boundary conditions and surface topography. In particular, we will consider the cases in which the cosinusoidal profile [Fig. 1(a)] of the grooved surface is replaced by a flat surface [Fig. 1(b)]. This approximation is usually valid when $qA \ll 1$. Also, we will solve the problem approximating the correct boundary conditions given by Eq. (6), and plotted in Fig. 1(c), with their Taylor expansions truncated to the first order [Fig. 1(d)].

We consider different cases in which we vary the ratio $A/\lambda=qA/2\pi$. We also introduce a reference anchoring energy $w=w_B$ given by Eq. (1), corresponding to the anchoring energy calculated from Berreman's approximation. The Laplace differential equation has been solved numerically [26], discretizing the specimen with 600 points per wavelength. The usual forward scheme has been used to calculate both space and time derivatives, and we have verified that the results are independent of the slab thickness and of the choice of the time step τ. As mentioned above, results are reported for the following four cases.

Case 1: flat profile on the bottom surface, with an approximate boundary condition

$$\theta_0(x) = \theta[x,z_0(x)] = -qA\,\sin(qx). \tag{11}$$

This case coincides with Berreman's analytical solution [1].

Case 2: flat profile on the bottom surface, with the exact boundary condition, Eq. (6).

Case 3: cosinusoidal profile on the bottom surface, with an approximate boundary condition, Eq. (11).

Case 4: cosinusoidal profile on the bottom surface, with the exact boundary condition, Eq. (6). This last case corresponds to the exact solution.

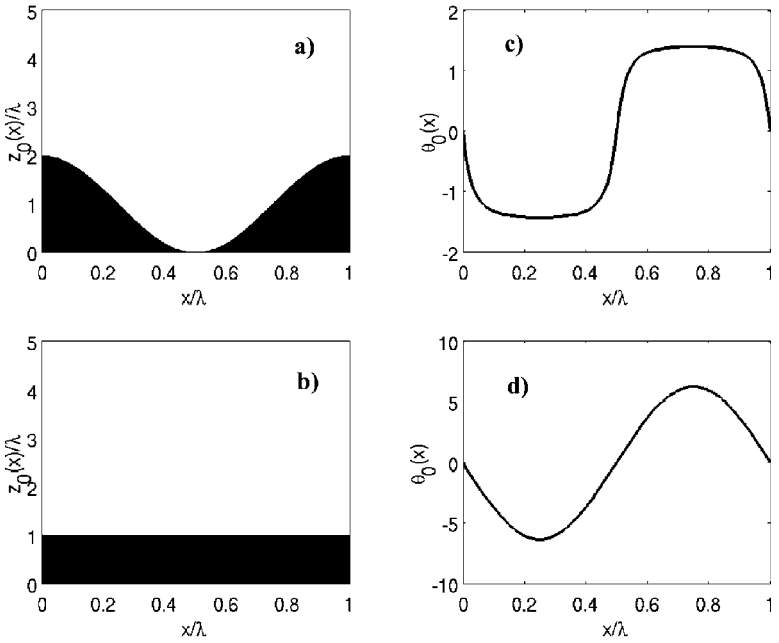

FIG. 1. Left column: Schematic representation for different approximations of the rubbed surface of the nematic cell. (a) Cosinusoidal profile described by Eq. (2); (b) flat surface. The two are equivalent in the limit $qA \ll 1$. Right column: Different boundary conditions for the anchoring direction of the director **n** indicating the nematic molecule orientation with respect to the x axes in the case of strong anchoring. (c) Exact boundary condition, given by Eq. (6); (d) its approximation derived as a Taylor expansion in qA truncated to the first order [Eq. (11)]. The two are equivalent when $qA \ll 1$.

We solve the bulk differential equation with the relevant boundary conditions for different values of A, ranging from 0 to λ. Note that both parameters K and λ are scaling parameters of the system, provided we scale the coordinates in λ units and normalize the energy to w_B. The parameter η in Eq. (9) is not relevant for the solution, provided it is sufficiently small to guarantee a slow convergence toward the equilibrium configuration.

The approximate solutions (cases 1–3) are expected to work well for small values of A. This is evident from the plots reported in Fig. 2, where maps of the equilibrium distribution of the elastic energy density $f=(1/2)K(\theta_{,x}^2+\theta_{,z}^2)$ are reported for the four cases considered. Very slight differences are present in the four images, the elastic energy density being always approximately uniformly distributed and concentrated in a very narrow zone close to the surface. On the contrary, when the depth of the grooves increases (Fig. 3 for $qA=3.0$), the solution for the three approximate cases is much different from the exact solution. Concentration of elastic energy density in correspondence with the positions in which the boundary conditions indicate horizontally aligned nematic molecules is evident in the bottom plots of Fig. 3

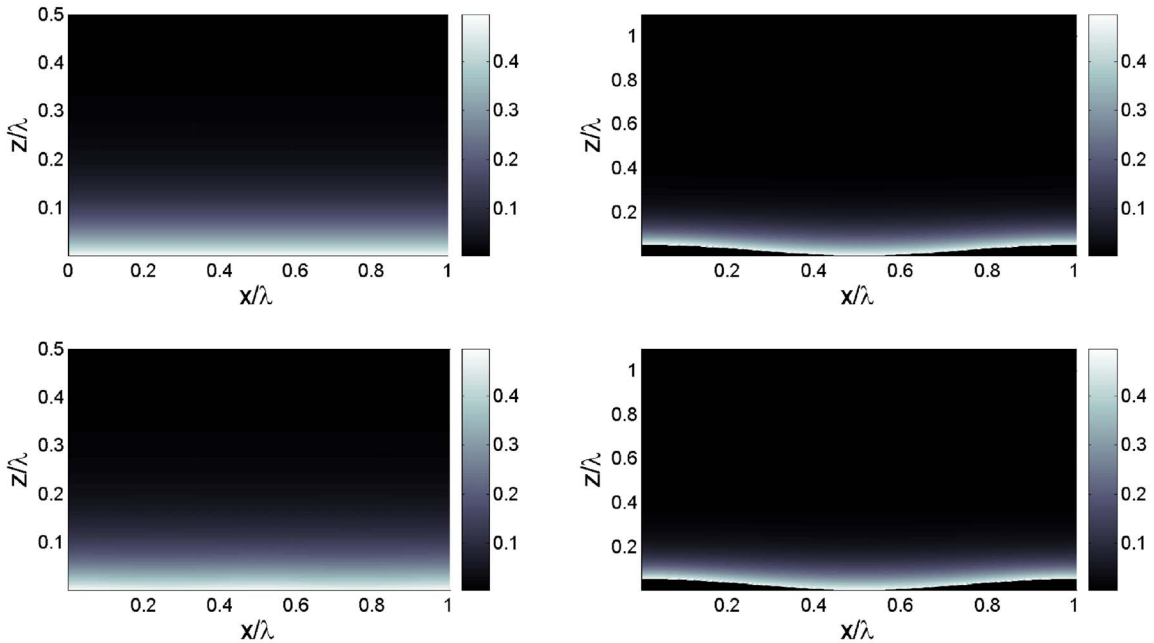

FIG. 2. (Color online) Distribution of the elastic energy density Eq. (3) when $qA=0.15$. Upper left: case 1 [flat surface with approximate boundary conditions (BCs)]; upper right: case 3 (exact surface with approximate BCs); lower left: case 2 (flat surface with exact BCs): lower right: case 4 (exact solution).

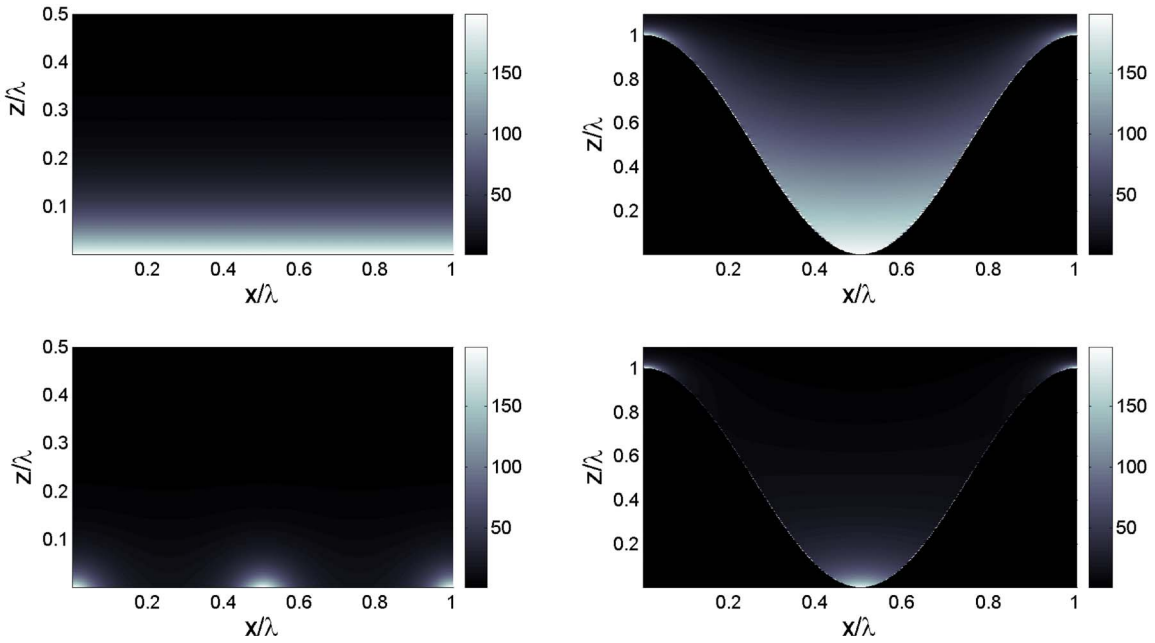

FIG. 3. (Color online) Distribution of the elastic energy density Eq. (3) when $qA=3.0$. Upper left: case 1 (flat surface with approximate BCs); upper right: case 3 (exact surface with approximate BCs); lower left: case 2 (flat surface with exact BCs): lower right: case 4 (exact solution).

(cases 2 and 4). Correspondingly, concentration of elastic energy density close to the maxima of the surface profile is also evident in the right plots of Fig. 3 (cases 3 and 4). A completely uniform solution is found, of course, in case 1 (upper left plot), equivalent to that for small A values (upper left plot of Fig. 2; note the different scales on the z axes).

It is interesting to observe that the solution in the case of a flat surface with the exact boundary conditions seems to better reproduce the exact total elastic energy of the system (space integral), while its spatial density distribution is better reproduced when the surface profile is not approximated and simplified boundary conditions are used.

This observation is confirmed in Fig. 4 where we plot the ratio $r=w/w_B$ vs qA. As expected, in the limit of small depth of the grooves ($A\to 0$), $r\to 1$, for the four cases considered. However, as soon as qA is of the order of 1, the exact solution deviates from Berreman's. In case 1, the calculated equivalent anchoring energy corresponds exactly to that calculated by Berreman. Approximation of the boundary conditions with their first-order Taylor expansion (case 2) corresponds to overestimating the equivalent anchoring energy, while considering the exact boundary conditions corresponds to an equivalent anchoring energy much smaller than that reported by Berreman. Indeed, the approximation of a flat surface provides reasonable results for all values of qA, with only a limited underestimation of the anchoring energy.

III. WEAK ANCHORING

We now extend the analysis of the previous section to the case where the anchoring energy on the interface solid-substrate–nematic-liquid-crystal is finite. The finite anchoring energy, taking into account the direct interaction of the nematic liquid crystal with the substrate, is assumed of the type [23]

$$g=-\frac{1}{2}w_e(\mathbf{n}\cdot\mathbf{t})^2=-\frac{1}{2}w_e\cos^2(\vartheta_s-\theta_0), \tag{12}$$

where w_e is the anchoring energy strength, and $\mathbf{n}$ and $\mathbf{t}$ the nematic director at the surface and the geometrical tangent of the profile, respectively. It follows that $\vartheta_s=\vartheta[x,z_0(x)]$. The nematic deformation is expected to be periodic with spatial period λ. The total energy of the sample, per period and for unit length along the y direction in the present case, is given by

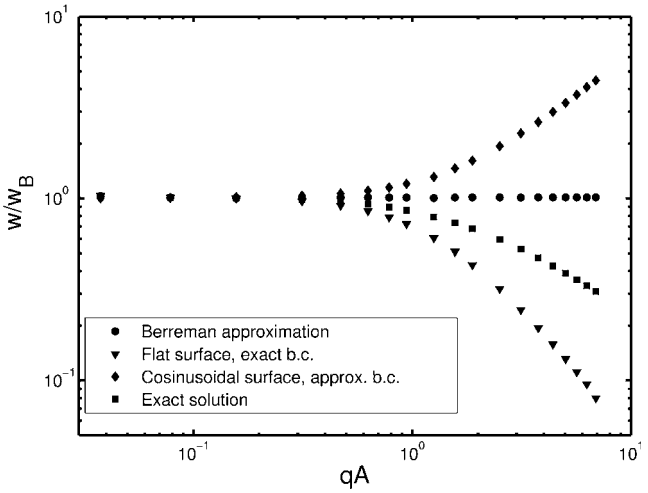

FIG. 4. Equivalent anchoring energy normalized to the value calculated by Berreman's analytical solution Eq. (1) as a function of qA. Strong anchoring at the surface.

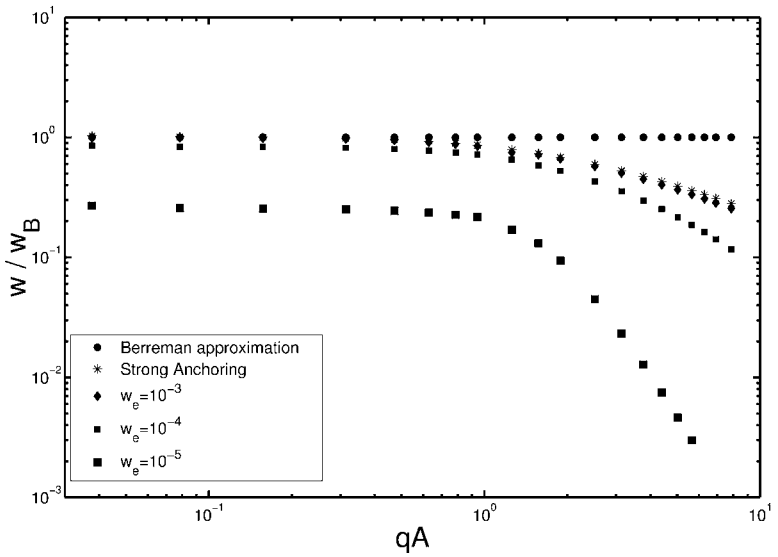

FIG. 5. Equivalent anchoring energy normalized to the value calculated by Berreman's analytical solution Eq. (1) as a function of qA. Comparison of the results with different anchoring strengths $w_e=\infty$, $2\pi\times10^{-3}$, $2\pi\times10^{-4}$, and $2\pi\times10^{-5}$.

$$F=\int_0^{\lambda}\int_0^{\infty} f[\theta(x,z)]dx\,dz+g[\vartheta_s(x)]. \tag{13}$$

The actual tilt angle $\theta(x,z)$ minimizing $F[\theta(x,z)]$ given by Eq. (13) is still a solution of the bulk Eq. (5), satisfying the condition of transversality (7) for $z\to\infty$, and on the solid surface described by Eq. (2). The boundary condition is [27]

$$K\{\sin\theta_0\ \theta_{,x}-\cos\theta_0\ \theta_{,z}\}+(w_e/2)\sin[2(\vartheta_s-\theta_0)]=0. \tag{14}$$

Equation (14) states that the elastic torque transmitted by the bulk to the surface is balanced by the surface torque due to the anisotropic interaction between the substrate and the nematic liquid-crystal molecules.

Again a numerical solution of the problem under consideration, relevant to weak anchoring, is possible by introducing a dynamic equation at the surface which replaces the boundary condition,

$$K\{\sin\theta_0\ \theta_{,x}-\cos\theta_0\ \theta_{,z}\}+(w_e/2)\sin[2(\vartheta_s-\theta_0)]=-\eta_s\theta_{s,t}, \tag{15}$$

in addition to the dynamical equation (9) for the bulk. In Eq. (15), η_s plays the role of surface viscosity [28]. In our numerical analysis we have verified that both Eqs. (9) and (15) converge to an equilibrium state solution.

Here we limit ourselves to showing the dependence of the equivalent anchoring energy w, defined by Eq. (10), on the amplitude of the grooves for different values of the anchoring energy w_e. Results are reported in Fig. 5 and indicate that the presence of weak anchoring introduces a further reduction of w with respect to the solution proposed by Berreman, as expected.

IV. CONCLUSION

Following the analysis proposed by Berreman, we have evaluated the effect of a modulated surface on the elastic energy of a nematic liquid crystal. The equivalent anchoring energy has been identified with the strain energy, per unit surface, of the nematic liquid crystal when the surface treatment forces the nematic molecules to be oriented perpendicular to the grooves. We have shown that the approximation introduced by Berreman to calculate the equivalent anchoring energy is correct only when the amplitude A of the grooves is much smaller than the wavelength of the profile of the limiting surface. For larger values of A, the anchoring energy estimated by approximating the strong anchoring at the boundary is overestimated with respect to the real anchoring energy of the nematic cell. Also, Berreman's solution overestimates the real equivalent anchoring energy when weak anchoring is present at the surface of the grooves.

Analytical solutions to the problem could be searched for in the form of a series expansion like Eq. (8). However, the usual orthogonalization procedures, which have to be carried out numerically, do not give monotonically decreasing coefficients M_n in order to assure the convergence of the series. For this reason, in our analysis, we have compared approximate solutions with the "exact" one, given by numerically solving the exact bulk equilibrium equation with the correct boundary conditions corresponding to strong and weak anchoring.

We note that further issues have to be considered, which involve nontrivial changes in the model equations, among them, the influence of the azimuthal director variations, the redefinition of the equivalent anchoring energy, necessary when the amplitude of the grooves is large, and the anisotropy of the elastic properties of the system. A detailed analysis of the related effects is beyond the scope of the present contribution.

[1] D. W. Berreman, Phys. Rev. Lett. **28**, 1683 (1972).
[2] P. G. de Gennes and J. Prost, *The Physics of Liquid Crystals*, Oxford Science Publications (Clarendon Press, Oxford, 1993).
[3] S. Faetti, Phys. Rev. A **36**, 408 (1987).
[4] J. B. Fournier and P. Galatola, Phys. Rev. E **60**, 2404 (1999).
[5] J. I. Fukuda, M. Yoneya, and H. Yokoyama, Phys. Rev. Lett. **98**, 187803 (2007).
[6] J. Cognard, Mol. Cryst. Liq. Cryst. Suppl. Ser.. **A5**, 1 (1982).
[7] J. Stöhr *et al.*, Science **292**, 2299 (2001).
[8] G. P. Bryan-Brown, C. V. Brown, I. C. Sage, and V. C. Hui, Nature (London) **392**, 365 (1998).
[9] C. J. Newsome, M. O'Neill, R. J. Farley, and G. P. Bryan-Brown, Appl. Phys. Lett. **72**, 2078 (1998).
[10] X. Lu *et al.*, Appl. Phys. Lett. **88**, 243508 (2006).
[11] F. S. Y. Yeung *et al.*, J. Appl. Phys. **99**, 124506 (2006).
[12] L. Komitov, G. P. Bryan-Brown, E. L. Wood, and A. B. J. Smout, J. Appl. Phys. **86**, 3508 (1999).
[13] G. P. Bryan-Brown, E. L. Wood, and I. C. Sage, Nature (London) **399**, 338 (1999).
[14] J. Haaren, Nature (London) **392**, 331 (1998).
[15] See, e.g., *Surfaces and Interfaces in Liquid Crystals*, edited by Th. Rasing and I. Musevic (Springer, Berlin, 2004), and references contained therein.
[16] W. M. Gibbons *et al.*, Nature (London) **351**, 49 (1991).
[17] M. Schadt, H. Seiberle, and A. Schuster, Nature (London) **381**, 212 (1996).
[18] M. Talarico, G. Carbone, R. Barberi, and R. Bartolino, Appl. Phys. Lett. **85**, 528 (2004).
[19] B. T. Hallam and J. R. Sambles, Liq. Cryst. **27**, 1207 (2000).
[20] P. Pagliusi, C. Y. Shen, and Y. R. Shen, J. Chem. Phys. **125**, 201104 (2006).
[21] D.-H. Chung *et al.*, Jpn. J. Appl. Phys., Part 1 **39**, 1252 (2000).
[22] D.-H. Chung, T. Fukuda, Y. Takanishi, K. Ishikawa, H. Matsuda, H. Takezoe, and M. A. Osipov, J. Appl. Phys. **92**, 1841 (2002).
[23] G. Barbero and L. Evangelista, *An Elementary Course on the Continuum Theory for Nematic Liquid Crystals* (World Scientific, Singapore, 2001).
[24] P. M. Morse and H. Feshbach, *Methods of Theoretical Physics* (McGraw-Hill, New York, 1953).
[25] G. Barbero and L. R. Evangelista, Phys. Rev. E **70**, 031605 (2004).
[26] G. Kaniadakis, P. P. Delsanto, and C. A. Condat, Math. Comput. Modell. **17**, 31 (1993); F. C. M. Freire, G. Barbero, and M. Scalerandi, Phys. Rev. E **73**, 051202 (2006).
[27] G. Barbero and G. Durand, J. Appl. Phys. **68**, 5549 (1990).
[28] A. I. Derzhanski and A. G. Petrov, Acta Phys. Pol. B **55**, 747 (1979).